Original Article

PROGRESS in MEDICAL PHYSICS Vol. 25, No. 4, December, 2014
http://dx.doi.org/10.14316/pmp.2014.25.4.193

Qualitative Evaluation of 2D Dosimetry System for Helical Tomotherapy

Sun Young Ma*, Tae Sig Jeung*, Jang Bo Shim†, Sangwook Lim*

*Department of Radiation Oncology, Kosin University College of Medicine, Busan,
†Department of Radiation Oncology, Guro Hospital, College of Medicine, Korea University, Seoul, Korea

The purpose of this study is to see the feasibility of the newly developed 2D dosimetry system using phosphor screen for helical tomotherapy. The cylindrical water phantom was fabricated with phosphor screen to emit the visible light during irradiation. There are three types of virtual target, one is one spot target, another is C-shaped target, and the other is multiple targets. Each target was planned to be treated at 10 Gy by treatment planning system (TPS) of tomotherapy. The cylindrical phantom was placed on the tomotherapy table and irradiated as calculations of the TPS. Every frame which acquired by CCD camera was integrated and the doses were calculated in pixel by pixel. The dose distributions from the fluorescent images were compared with the calculated dose distribution from the TPS. The discrepancies were evaluated as gamma index for each treatment. The curve for dose rate versus pixel value was not saturated until 900 MU/min. The 2D dosimetry using the phosphor screen and the CCD camera is respected to be useful to verify the dose distribution of the tomotherapy if the linearity correction of the phosphor screen improved.

Key Words: Tomotherapy, Phosphor screen, Dose distribution, Blur kernel, Gamma index

Introduction

A CT (computed tomography) shaped TomoTherapy Hi Art unit delivers radiation using a helical tomotherapy technique. A small sized linear accelerator is installed on a ring gantry that continuously rotates while the treatment table is moving along the axis of gantry rotation during irradiation. The beam has fan geometry and 64 leaf binary collimators are used to subdivide this fan beam into beamlets. Intensity modulation is achieved by a temporal modulation of the collimator leaves. The unit is designed for intensity modulated treatment delivery. The tomotherapy unit takes advantage of a field flattening filter free. The advantage of this design is a relatively high dose rate and a radiation field that varies less in energy across the field.[1] Conventional dosimetry methods as well as 3D water phantom are not applicable to this unit.[2] Therefor, many methods to verify the tomotherapy has been developed such as diode array detector.[3-6] In this study, the cylindrical water phantom was fabricated and the phosphor screen was used, since it is sensitive to the therapeutic radiation and we can observe the radiation in real-time.[7,8]

The aim of this study is to see the feasibility of the 2D (dimensional) dosimetry system using phosphor screen for helical tomotherapy.

Materials and Methods

A custom made cylindrical water-filled phantom with a phosphor screen (LANEX Fast Screen, Kodak, USA) was designed to see the real-time dose distribution of the tomotherapy. The phosphor screen with 18 cm diameter was placed axially in the cylindrical water-filled phantom and faced toward the lens of the charge-coupled device (CCD) camera

This research was supported by Basic Science Research Program through the National Research Foundation of Korea (NRF) funded by the Ministry of Education, Science and Technology (2010- 0013701 and 2013R1A1A2012013).
Received 20 October 2014, Revised 29 October 2014, Accepted 24 November 2014

Correspondence: Sangwook Lim (medicalphysics@hotmail.com)
Tel: 82-51-990-6393, Fax: 82-2-6280-6247

(SAERIM, Korea) as shown Fig. 1. The outer diameter of the phantom is 25 cm. The phosphor screen in the phantom is to emit visible light during it irradiated. The water on either side of the screen provided 20 cm of side scatter. The CCD camera captured the fluorescent light from the screen through the optical glass window of the phantom during irradiations from the tomotherapy unit.

In order to evaluate the 2D dosimetry system for tomother-

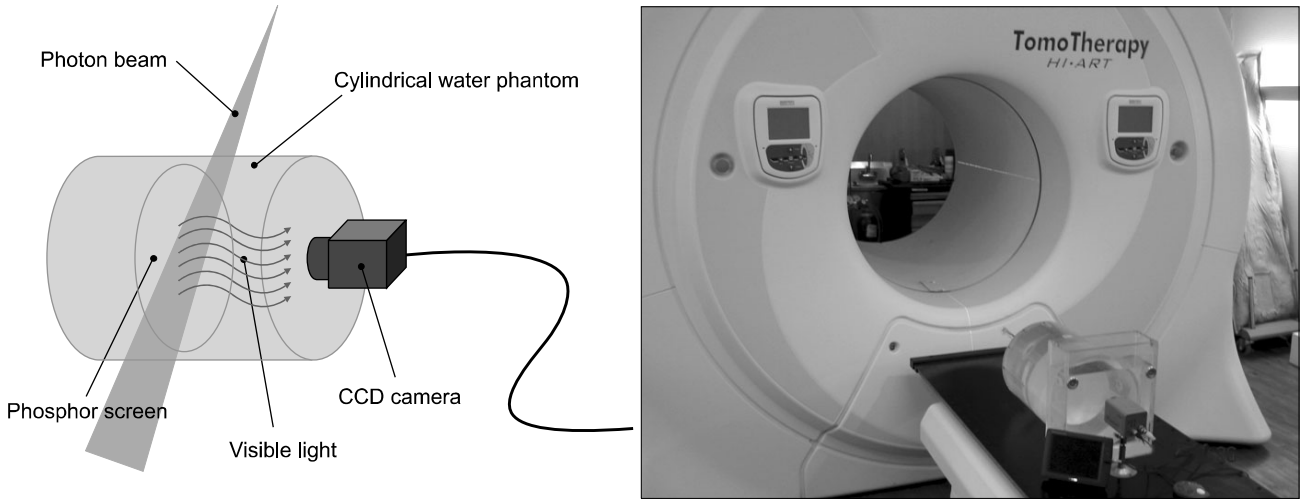

Fig. 1. Custom made cylindrical water phantom for tomotherapy: The phosphor screen placed axially in the phantom and the CCD camera captures the visible light from the phosphor screen during the irradiation. The LCD monitor is used to check the focus and the setup of the phantom and the CCD camera.

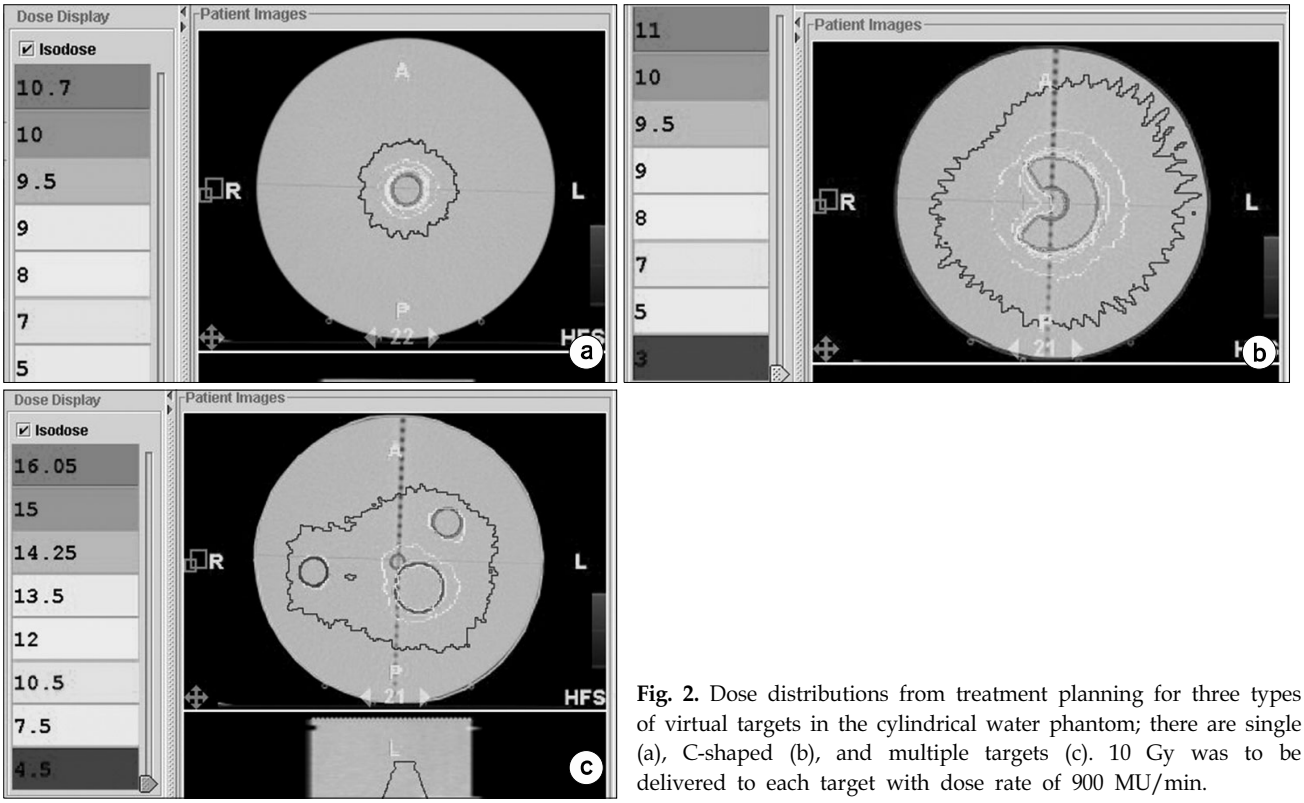

Fig. 2. Dose distributions from treatment planning for three types of virtual targets in the cylindrical water phantom; there are single (a), C-shaped (b), and multiple targets (c). 10 Gy was to be delivered to each target with dose rate of 900 MU/min.

apy developed in this study, three types of radiation treatment planning-single, c-shaped, and multiple targets-were created in the cylindrical water phantom (Fig. 2). 10 Gy was to be delivered to each target with dose rate of 900 MU/min.

The phosphor screen was exposed to the 6 MV photon beam from the linac and the tomotherapy. The CCD camera captured the fluorescent light from the screen at 29.9 frames per second during the irradiation. The motion images from the CCD camera were sent to the frame grabber and the images were digitized into MPEG4 format as 720×480 pixel size and 8 bit gray scale in real-time. The computer corrects and integrates the frames for measuring 2D dose distributions (Fig. 3).

Cylindrical water phantom without the phosphor screen was irradiated 6 MV photon beam to subtract the background which caused by light leakage and CCD of the camera itself. In order to obtain the correction factors for the dose rate, the phosphor screen in the phantom was calibrated at the reference conditions; at SAD 80 cm with 10×10 cm^2 field size for linac, center of the gantry ring with 5×40 cm^2 field size for the tomotherapy. The energy dependency was investigated by measuring the depth dose and irradiating of various photon energies. Increasing the dose rate from 100 MU/min to 900 MU/min at 100 MU/min step, the frames were cumulated and measured the pixel values at the same depth. The dose rate dependency was applied to each frame.

In order to measure the blurring effect on the captured images, small point field was delivered on the screen. Off-axis profile for the point plotted to obtain the blurring kernel. V_0 is

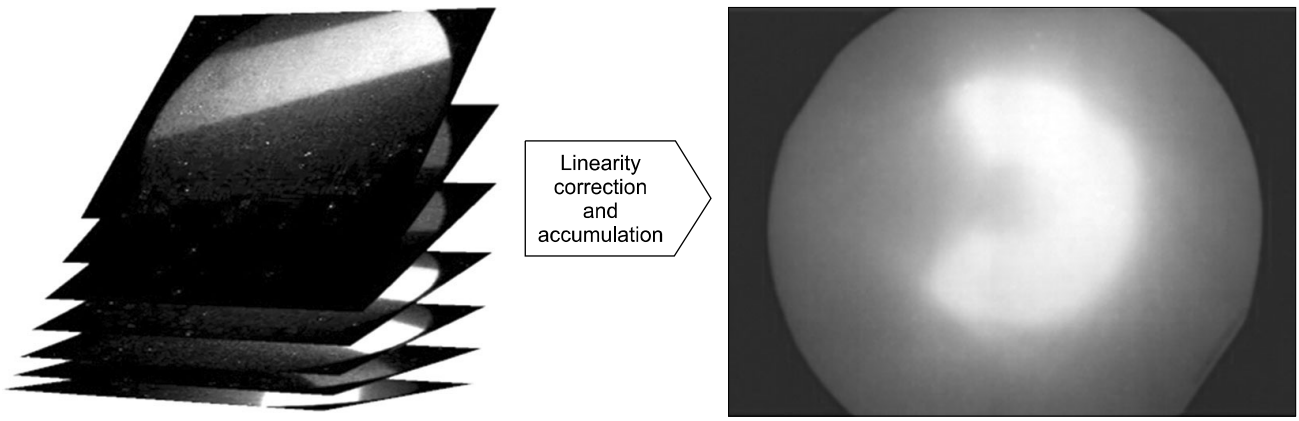

Fig. 3. Every frame were calibrated and cumulated. Right picture shows example of reconstructed dose map for C-shaped virtual target.

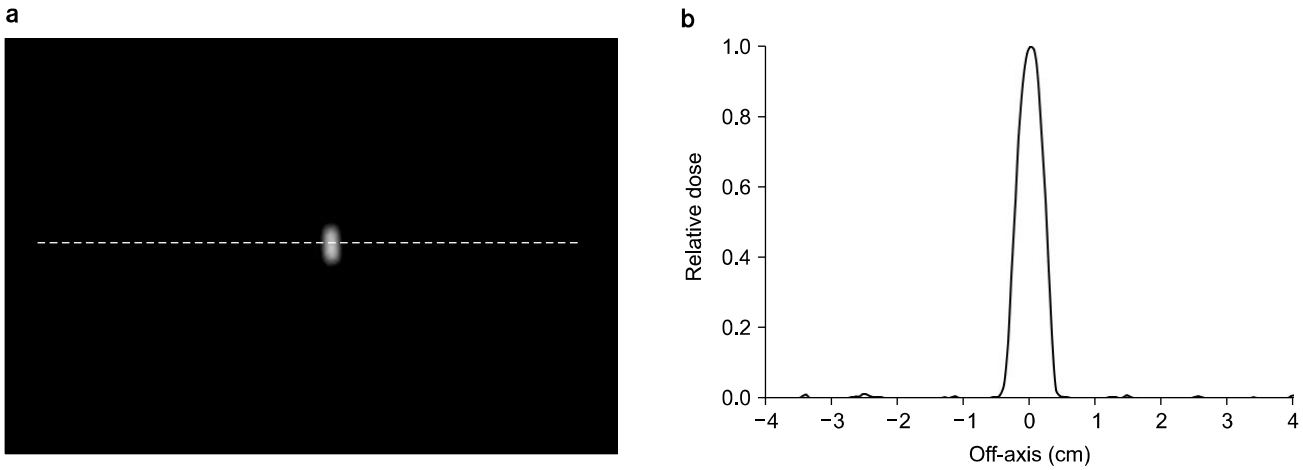

Fig. 4. Profile of point dose from phosphor screen: (a) shows the point radiation on the phosphor screen. Blurring kernel (k) was obtained from the profile (b).

pixel value without blurring effect and V is measured pixel value (Fig. 4). The blurring kernel k was obtained by Gaussian fitting. The deconvolution of the Gaussian function was applied to the pixel values of each frame before they reconstructed.

$$V = V_0 \otimes k \quad (1)$$

The virtual targets were assumed to be in the CT images of the phantom, which were planned and treated. There are three types of target, one is one spot target, another is C-shaped target, and the other is multiple targets. Each target was planned to be treated at 10 Gy by treatment planning system (TPS) of tomotherapy. The cylindrical phantom was placed on the tomotherapy table and irradiated as calculations of the TPS. Every frame was integrated and the doses were calculated in pixel by pixel. The point dose was measured with an ion-chamber in the phantom to convert the relative dose to absolute one. The dose distributions obtained from the phosphor screen were compared with those calculated from the TPS. During irradiation, the fluorescent light captured by the CCD camera (29.9 fps) was transferred to the computer to be analyzed and displayed. The dose distributions of the fluorescent images were compared with the calculated dose distribution from the TPS. The discrepancies

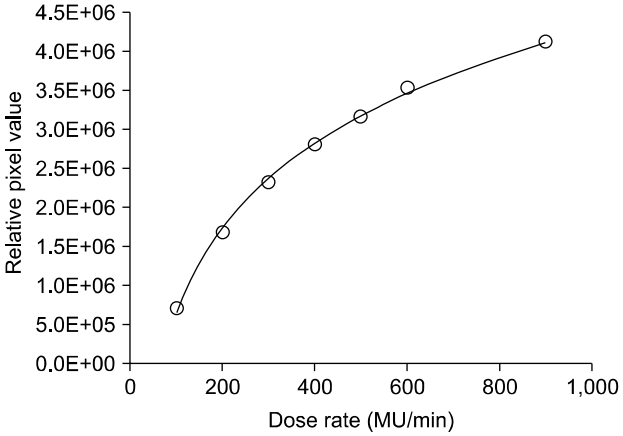

Fig. 5. Dose rate dependency; the relative pixel values were measured versus dose rates from 100 MU/min to 900 MU/min. The solid line and the dotted line are the measurements and the fitting, respectively.

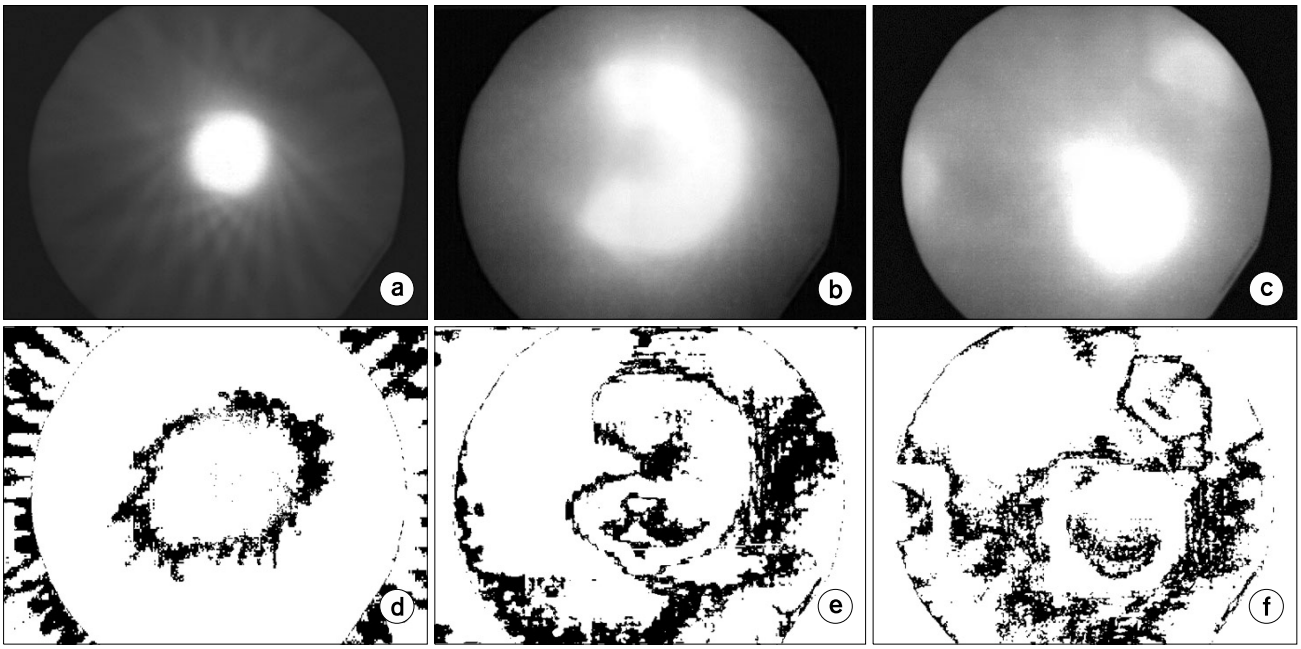

Fig. 6. The dose distributions for three cases of virtual targets were analyzed. (a), (b), and (c) are cumulated gray scale images for single target, C-shpaed target, and multiple targets, respectively. (d), (e), and (f) are the gamma evaluation map between calculated and measured doses for three types of target. (d), (e), and (f) are the gamma evaluation map between calculated and measured dose distributions for three types of target. The pass rates are 84.46%, 80.38%, and 83.28%, respectively.

were evaluated as gamma index by using the custom software built with IDL 6.3 (Exelis VIS, inc, Boulder, CO, USA) for each treatment.

Results

The pixel values were measured at the dose rates from 100 MU/min to 900 MU/min at the reference condition. The intensity of visible light depends on the dose rate and the energy of the radiation as show Fig. 5. The gray scale images relative to dose can be observed during the irradiation.

Fig. 6 shows the dose distributions for three cases of virtual targets. (a), (b), and (b) are cumulated gray scale relative to the dose images for single target, C-shpaed target, and multiple targets, respectively. (d), (e), and (f) are the gamma evaluation between calculated and measured dose distributions for three types of target, respectively.

Comparing the dose distribution from the TPS, the calculated and the measured dose distributions showed a good agreement at over 80% dose region. The results of 2D gamma evaluation show that the large discrepancies distributed at low dose region. The pass rates for three virtual targets were 84.46%, 80.38%, and 83.28%, respectively.

Discussion and Conclusion

The integrated pixel values were relative to the number of frames. And also the dose was relative to the number of frames (29.9 fps). The dose rate was affect to the pixel values rather than the radiation energies. It is obvious the curve of dose versus pixel value is linear. Therefore, the linearity correction for dose versus pixel value was not needed.[9] The curve for dose rate versus pixel value was not saturated until 900 MU/min. It is feasible the phosphor screen for measuring the dose of therapeutic radiation. However, the results were not shown in this study, the energy dependency for spread function in this system was reported not significant for 6 MV and 15 MV photon beams.[9] It seems that the dose distribution error between the calculation from the TPS and the measured by this system was caused by light scattering effect in the water. Further study will be focused on the light scattering effect in the water. The energy dependency in this system was ignorable. The large discrepancies at low dose region seem caused by that the scintillator was sensitive to the scattered photon beams.

However, the measured dose distributions were similar to the calculated dose distributions in qualitative. The discrepancies in the low dose region were larger than central region. It seems that the phosphor screen is sensitive for the scattered radiation and we need to improve the linearity correction methods. In this study, the gamma evaluations outside of the rounded phosphor screen region should be ignored in the gamma maps. For the single target in Fig. 6d, if the gamma evaluation outside of the region were ignored, the pass rate would be increased.

The phosphor screen is easy to handle and reusable for dosimeter in radiotherapy. The characteristic of the screen is feasible to apply to the therapeutic radiation as long it is well calibrated. 2D dose distributions of the other slices in the phantom could be evaluated by moving the phosphor screen or the phantom in a longitudinal direction. A real-time 2D dosimetry using the phosphor screen and the CCD camera is respected to be useful to verify the dose distribution of the tomotherapy. Further study will be concerned on the 3D dosimetry of the tomotherapy by fixing the phantom in the middle of the gantry ring.

References

1. Welsh JS, Patel RR, Ritter MA, et al: Helical tomotherapy: an innovative technology and approach to radiation therapy. Technol Cancer Res Treat 1(4):311-316 (2002)
2. Langen KM, Papanikolaou N, Balog J, et al: QA for helical tomotherapy: Report of the AAPM Task Group 148. Med Phys 37(9):4817-4853 (2010)
3. Langen KM, Meeks SL, Poole DO, et al: Evaluation of a diode array for QA measurements on a helical tomotherapy unit. Med Phys 32(11):3424-3430 (2005)
4. Geurts M, Gonzalez J, Serrano-Ojeda P: Longitudinal study using a diode phantom for helical tomotherapy IMRT QA. Med Phys 36(11):4977-4983 (2009)
5. Feygelman V, Opp D, Javedan K, et al: Evaluation of a 3D diode array dosimeter for helical tomotherapy delivery QA. Med Dosim 35(4):324-329 (2010)
6. Pavoni JF, Pike TL, Snow J, DeWerd L, Baffa O: Tomotherapy dose distribution verification using MAGIC-f polymer gel dosimetry. Med Phys 39(5):2877-2883 (2012)
7. Lim S, Yeo IJ, Kim DY, Ahn YC, Huh SJ: Application of an imaging plate to relative dosimetry of clinical x-ray beams. Kor J Med Phys 11(2):117-122 (2000)

8. **Lim S, Yi BY, Ko YE, et al**: Feasibility study of the real-time IMRT dosimetry using a scintillation screen. J Korean Soc Ther Radiol Oncol 22(1):64-68 (2004)

9. **Li JS, Boyer AL, Ma CM**: Verification of IMRT dose distributions using a water beam imaging system. Med Phys 28(12):2466-2474 (2001)

2차원 토모테라피 선량측정시스템의 정성적 평가

*고신대학교 의과대학 방사선종양학교실, †고려대학교 구로병원 방사선종양학과

마선영* · 정태식* · 심장보† · 임상욱*

본 연구의 목적은 새로 개발된 2차원 토모테라피 선량측정 시스템의 가능성을 알아보는 것이다. 방사선이 조사되면 가시광성을 내보내는 인광판을 원통형 물팬텀에 삽입하였다. 치료계획장치에서 원 모양, C자 모양, 다중표적 3종류의 가상의 표적을 만들고 각 표적에 10 Gy의 방사선을 전달하도록 하였다. 원통형 팬텀을 토모테라피 치료테이블위에 올려놓고 치료계획대로 방사선을 조사하였다. CCD카메라로 촬영된 모든 프레임은 누적되었고 각 픽셀은 선량으로 변환되었다. 인광판으로부터 나온 영상은 치료계획장치에서 계산된 선량분포와 비교하였다. 선량기울기(dose rate)와 픽셀값의 관계 그래프는 선량기울기 900 MU/min 까지 포화(saturated)되지 않았다. 인광판의 선형성 보정이 개선된다면 인광판과 CCD 카메라를 이용한 토모테라피의 2차원 선량측정이 유용할 것으로 기대한다.

중심단어: 토모테라피, 인광판, 선량분포, 흐림커널, 감마지수